

## Journal of Stress Analysis

Vol. 8, No. 1, 2023-24, 57-67



ORIGINAL RESEARCH PAPER

## Electroplastic Effect on the Formability of Annealed AA6-061 in Equibiaxial Tension Stress State

Amirhesam Farkhondeh, Mohammad Bakhshi-Jooybari<sup>\*</sup>, Hamid Gorji, Mohammad Javad Mirnia

Faculty of Mechanical Engineering, Babol Noshirvani University of Technology, Babol, Iran.

### Article info

Article history:
Received 18 July 2023
Received in revised form
13 September 2023
Accepted 21 September 2023

Keywords:
Electro assisted forming
Electroplasticity
Electroplastic effect
Formability
Al6061
Hydraulic bulge test

#### Abstract

The use of electric current is an innovative technology in forming processes. Considering the vital role of forming processes in various industrialized applications and the wide utilization of light metal alloys, especially AA6061 aluminum alloy sheets, it is important to examine the electroplastic effect on the formability of AA6061 in different stress states. In this article, the electroplastic effect on the formability of AA6061 sheets in the states of annealing heat treatment and in equibiaxial tension stress states is investigated by the hydraulic bulge test. The appropriate current parameters were first determined from a set of parameters. The results showed that due to the utilization of electric pulses at appropriate current parameters, the fracture pressure was reduced by 6.67%, and the dome height of the bulge was increased by 5.52%. Moreover, by investigating the thickness distribution, the bulge dome thickness was decreased by 6.9%. This shows that in the equibiaxial tension stress state, when the electric current was applied at appropriate current parameters, the formability increased and the forming force decreased. Through theoretical calculation of the biaxial stress curve in terms of thickness strain, it was observed that by applying the electric current at appropriate current parameters, the formability of the sample increased, and the forming force decreased. As a result, the theoretical results confirmed the experimental results. The results of this study can be used as a basis for the application of the electroplastic effect to more complex stress states and finally using the electroplastic effect in the industry.

### Nomenclature

$\varepsilon_D^{-pl}$	Plastic strain at the threshold of fracture	$\eta$	Stress triaxiality
$\xi(\theta)$	Lode angle	$\varepsilon^{-pl}$	Equivalent plastic strain
$\varepsilon_1$	Maximum plane strain	$arepsilon_2$	Minimum plane strain
a	Major diameter of the ellipse (mm)	b	Minor diameter of the ellipse (mm)
$h_b$	Bulge height (mm)	p	Bulge pressure (bar)
Rf	Blank holder fillet radius (mm)	$t_0$	Sheet initial thickness (mm)
$d_d$	Die cavity diameter (mm)	$R_b$	Bulge radius (mm)

<sup>\*</sup>Corresponding author: M. Bakhshi-Jooybari (Professor)

E-mail address: bakhshi@nit.ac.ir doi 10.22084/JRSTAN.2024.29624.1260

ISSN: 2588-2597



β	The ratio of maximum and minimum	d	The initial diameter of the circle engraved
	plane strains		on the sample (mm)
$ar{arepsilon}_b$	Effective biaxial strain	$  \bar{\sigma}_b  $	Effective biaxial stress (MPa)
$\mid t \mid$	Dome apex sheet thickness (mm)		

### 1. Introduction

Over recent years, there has been a growing demand for new technologies that enhance the complexity of product shapes across various material categories [1]. Lightweight materials such as aluminum alloys are commonly used in manufacturing processes [2]. The use of these alloys has caused a grow in the fuel efficiency of automobiles [3]. However, despite the numerous advantages resulting from the use of aluminum alloys as structural elements, their formability at low temperatures is inadequate. To meet these requirements, new technologies have been evolved to enhance the formability of materials [4]. Traditionally, the enhancement of material formability could be achieved through two main approaches: mechanical strategies and thermal fields [5, 6]. Mechanical strategies involve the utilization of incremental processes and non-linear deformation paths [7, 8]. On the other hand, thermal fields refer to techniques such as hot forming or localized temperature-supported processes [4]. A novel approach to enhancing the formability of metal alloys involves the utilization of electrical current. In this process, direct current (DC) or alternating current (AC) is applied to the part to increase the formability of the material and to reduce the forming force [9]. Numerous studies have reported that applying an electric current (particularly pulsed current) to a metal while it is being deformed can significantly increase its formability [10]. The cause of this phenomenon is called electroplastic effect [11]. Roth et al. [12] observed that the elongation of AA5754 sheet could be increased more than four times during pulsed electro assisted uniaxial tensile test. Heigel et al. [13] observed that the application of electrical pulses to the 6061-T6 aluminum sheet, both prior to and during deformation in the uniaxial tension test, had the potential to decrease the amount of energy required for forming and the flow stress. Salandro et al. [14] observed that the application of electrical pulsing to 5052 and 5083 aluminum alloys during uniaxial tensile test resulted in an increase in elongation and a decrease in the engineering yield stress. Pleta et al. [15] observed that the application of electrical pulses to an AA5083 aluminum alloy sheet during uniaxial tensile test reduced anisotropy, restricted the formation of Lüder's bands, and enhanced formability. Kim et al. [16] stated that the application of electrical pulses to AA5052-H32 aluminum alloy sheet samples in uniaxial tensile tests caused a notable growth in the alloy's elongation. Roh et al. [17] conducted research on the influence of electrical pulses on the formability

of AA5052-H32 aluminum alloy sheets in a quasi-static tensile test with different sets of two electric pulses parameters, the pulse period and the electric energy density. It was observed that by appropriately selecting these parameters, the formability of this alloy experienced a significant improvement at room temperature. Hong et al. [18] noticed an improvement in the strain and a decrease in the force during forging a 6061-T6 aluminum alloy by applying electrical pulse. Moreover, they concluded that because of the electroplastic effect, several benefits were present when applying electrical pulses to the metal forming processes such as rolling [19] or drawing [20]. Zhao et al. [21] observed that by applying electrical pulses to AA5754 aluminum alloys in a uniaxial tensile test, the utilization of electrical pulses led to a rise in temperature and a decrease in yield stress. In addition, the total elongation increased with higher current density. Shaffer et al. [22] examined the effect of applying electric pulses for the purpose of electrical treatment after deformation and heat treatment to AA2024 aluminum alloys. It was observed that applying electric pulses did not have a significant effect on the microstructure, compared to heat treatment, and led to an improvement in formability. Ghiotti et al. [23] examined the electroplastic effect on the formability of AA1050 sheet samples in uniaxial tensile test under varying current densities and stress states. They reported that the electroplastic effect was seen in all stress states and that the electroplastic effect on formability decreased with the increase in the stress triaxiality. They also observed that at different stress triaxialities, the appropriate current intensity was constant. Simonetto et al. [24] demonstrated that applying DC to the AA1050 sheet in under H24 condition had a more pronounced effect than under the annealed condition. Additionally, other studies have highlighted varying electroplastic effects on the material behavior in different hardening states for aluminum alloys 5xxx [25], 6xxx [26], and 7xxx [27]. Xu et al. [28] observed that applying electrical pulses to AZ31 magnesium foils during uniaxial tensile tests significantly increased formability. This is attributed to the increase in the speed of movement of dislocations due to the application of electric pulse. Eslami et al. [29] investigated the electroplastic effect on the formability of aluminum alloy 6061 through uniaxial tensile test. They found that applying electric pulses led to improved formability. Farkhondeh et al. [30] investigated the electroplastic effect on the AA6061 formability under two heat treatment conditions, T6 and annealing, through uniaxial tensile test. They found that

applying electric pulses under appropriate current parameters during both heat treatment states improved formability. The improvement rate was 23.4% in the annealed state and 5.7% in the T6 state. By qualitative analysis of the microstructure using the scanning electron microscope (SEM) images of the fracture surface, it was observed that this phenomenon could be attributed to an augmentation in the size and number of fracture surface dimples under the annealed condition, compared to the T6 condition. Furthermore, the application of electric current with appropriate parameters to the annealed sample intensified the size and the number of the dimples and increased the formability.

In the studies reviewed in this field, investigation of the electroplastic effect on the plastic behavior of AA6061 aluminum alloy sheets is limited to only a few articles. In these articles, only the electroplastic effect on the plasticity of this alloy in the state of uniaxial tension stress was investigated. The purpose of investigating the electroplastic effect on the plasticity of AA6061 sheet is to use this effect in the industry to improve the production. Since the stress states in the industry are more complex than in the uniaxial tension, there is a lack in investigating the electroplastic effect in other stress states through more complex tests. Given the critical role of forming processes in various industrial applications and the wide use of light metal alloys, especially AA6061 aluminum alloy sheets in various industries, low formability of these alloys at low temperatures is considered as a challenge. According to the studies, the use of electric current in the industry could solve this problem. In addition, the superiority of this method over heat treatment is that it does not affect the microstructure of the sample and increases the formability. It should also be noted that in order to industrialize this technique, the electroplastic effect on the formability of the sample in different stress states must be determined first. Therefore, it is important to examine the effect of electroplastic on the formability of AA6061 sheets in different stress states. Now, as the hypotheses of this study, the question is raised whether the electroplastic effect on formability changes in different stress states. If it does, how?

In order to answer these hypotheses, the objectives of this study are as follows:

- The electroplastic effect on the formability of annealed AA6061 sheets in stress state of equibiaxial tension is investigated using the hydraulic bulge test.
- Then, by analyzing the circular pattern created on the sample, the fracture parameters at the bulge dome are obtained, and the effect of stress state on the formability in electroplastic forming is examined.

Innovation topics of this research compared to the

above examined articles are as following:

- Due to the lack of studies on the electroplastic effect on the formability of AA6061 in more complex stress states, investigating the electroplastic effect on the formability of annealed AA6061 in equibiaxial stress state represents a novel research topic.
- To investigate the electroplastic effect on the formability of AA6061 in the equibiaxial stress state, the hydraulic bulge test was performed. According to the reviewed articles, the uniaxial tensile test was used to investigate the electroplastic effect in other stress states. Therefore, investigating the electroplastic effect by means of the hydraulic bulge test, which is a more complex test compared to the uniaxial tensile test, can be considered as one of the innovations of this research.
- Rather than focusing just on DC, this study investigates the electroplastic effect using AC in the form of sinusoidal waveform considering various current parameters.

#### 2. Materials and Methods

AA6061-T6 sheets with a thickness of 1mm was used for this research. Table 1 shows the chemical composition of the sheets. In order to reduce thermal effects during the tensile tests, an electric current was applied using a pulsed current generator. The generator and the schematic of its main components are shown in Fig. 1. This device is capable of producing sinusoidal pulsed currents with a maximum current intensity of 500 A. The important parameters of this device are listed in Table 2.

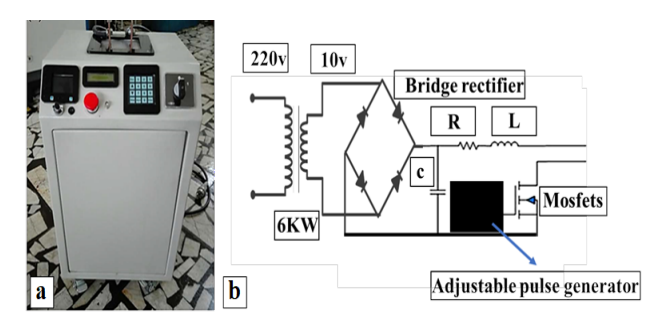


Fig. 1. Electric current generating device: a) generator b) circuit.

Table 1 Chemical composition of Al 6061-T6 sheets used in the experiments (wt.%).

Al	Mg	Fe	Mn	Ti	Si	Cu	$\operatorname{Cr}$	Zn
Remainder	0.9	0.3	0.02	0.01	0.69	0.25	0.16	0.02

 Table 2

 Important parameters of the sinusoidal pulse current generator.

Current	Pulse duration	Pulse period	Frequency
(A)	$(10^{-3} \text{ s})$	(s)	(Hz)
0-500	0.06,0.12,0.24,0.4	0.001-10	0.1-1000

In order to investigate the electroplastic effect in the equibiaxial tension stress state by means of the hydraulic bulge test in annealed heat treatment state, the samples were prepared according to Fig. 2 using a wire cut machine. Two holes with the diameter of 5mm were created to connect the electrodes of the pulsed current generator to the sample by screws. After preparing the sample for experimental analysis, to obtain the fracture parameters on the sample, a circular pattern with a 2-mm diameter was made using the chemical etching method. For additional details on calculating failure parameters, refer to Section 3.2.

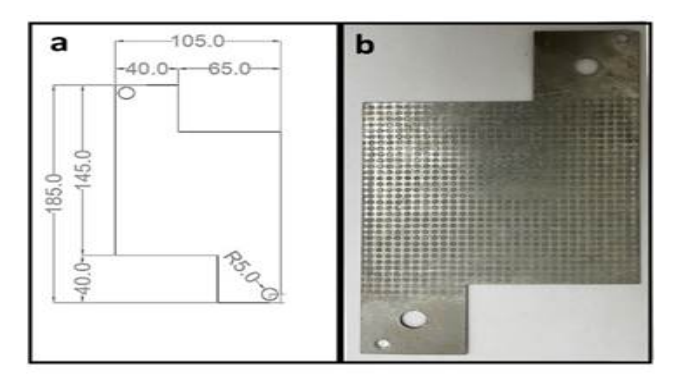


Fig. 2. Hydraulic bulge test sample.

The schematic of hydraulic bulge test is shown in Fig. 3. The main variables of this test are sample dome bulge height  $(h_b)$ , bulge pressure (p), dome apex sheet thickness (t), and sample bulge radius  $(R_b)$ . The fixed parameters are blank holder fillet radius  $(R_f)$ , sheet initial thickness  $(t_0)$ , and die cavity diameter  $(d_d = 2R_d)$  [31].

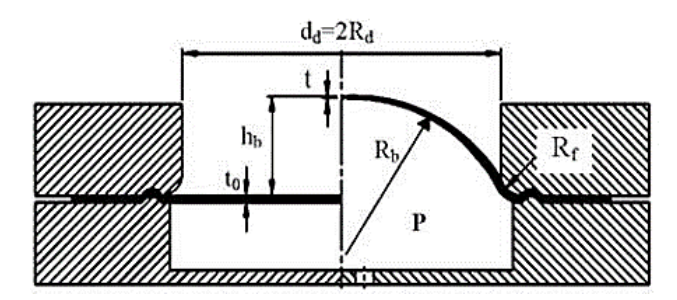


Fig. 3. Schematic of hydraulic bulge test [31].

The die used in the hydraulic bulge test was made of CK45, whose image is displayed in Fig. 4a. According to Fig. 4b, the diameter of the blank holder is 56mm and the screws used in this die are made of M12. The general schematic of the electro assisted hydraulic bulge test is shown in Fig. 5. In order to insulate and seal the sample with the blank holder, a 3mm thick

polyurethane sheet was used. Due to the high plasticity of the sample under the electroplastic effect, the polyurethane sheet could tear earlier than the sample and lose its effectiveness. Thus, a 0.1-mm thick SS304 sheet was placed on top of the polyurethane sheet. Then, the sample was positioned on the stainless-steel sheet. Finally, another 0.1-mm thick polyurethane sheet was used to insulate the sample within the die. A Mitutoyo 500-197-20 digital caliper was used to measure the height of the bulge. This device has the ability to measure with an accuracy of 0.01mm which is fixed on the die according to Fig. 5. With this caliper, it was possible to read the sample dome bulge height online until the moment of fracture. In order to read pressure, a hand manometer was used which was placed before the fluid entered the blank holder. After connecting the electric current to both sides of the sample, the hydraulic oil entered the die, and the test was continued until the moment of sample fracture. During the tests, a video was being recorded, and once the test was finished, the dome bulge height and the corresponding pressure were recorded by watching the video.

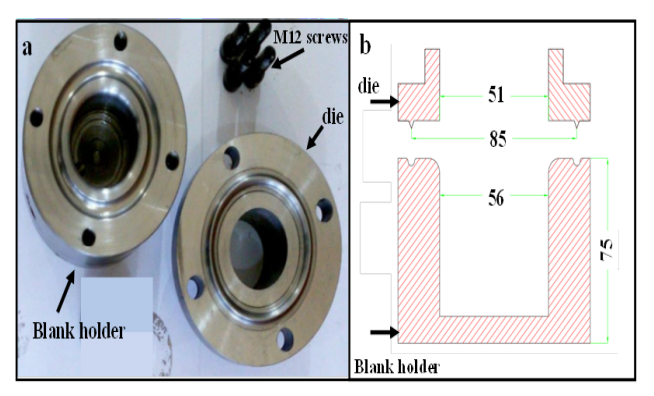


Fig. 4. Hydraulic bulge test die set.

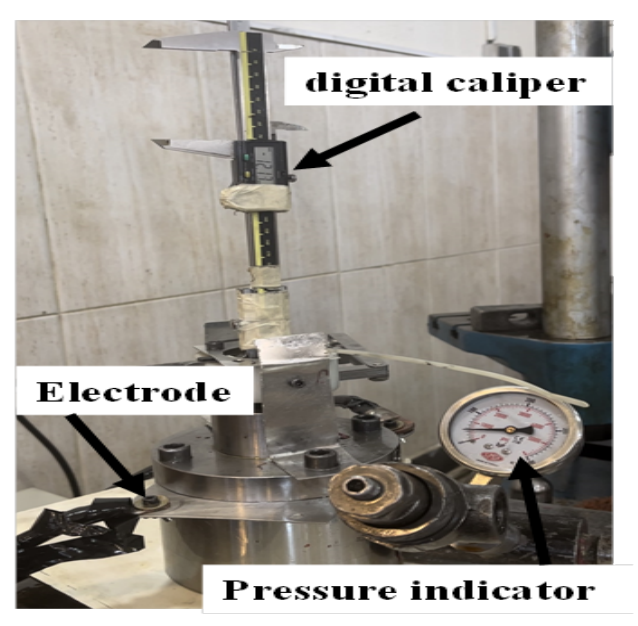


Fig. 5. Hydraulic bulge test setup.

### 3. Results and Discussion

# 3.1. Appropriate Current Parameters in the Equibiaxial Tension Stress State

In our previous study [30], the electroplastic effect on the formability of AA6061 sheets under two heat treatment conditions of T6 and annealed was investigated using uniaxial tensile tests. In that study, the appropriate current parameters for both heat treatment conditions were found within a set of parameters. The set of parameters were identified based on the articles reviewed, available facilities of the laboratory, and the experience obtained in the Advanced Material Forming Research Center of Babol Noshirvani University of Technology. Finally, in that study the appropriate current parameters were the same for both conditions. These parameters are shown in Table 3.

**Table 3** Appropriate current parameters in uniaxial tension stress state, type of current: Sinusoidal.

Current intensity	Pulse duration	Pulse period
(A)	$(\mu \mathrm{s})$	(ms)
360	20	120

To ensure that the appropriate current parameters in the stress state of equibiaxial tension were the same as those of the stress state of uniaxial tension, hydraulic bulge tests were performed as follows. Initially, in the state without applying an electric current, the bulge test was performed and the bulge fracture height was recorded by a digital caliper. Next, with the appropriate current parameters determined from the uniaxial tension stress state, the bulge test was performed. Subsequently, additional bulge tests were conducted at different current intensities; at a higher current intensity (460A), and at a lower current intensity (260A), compared to that of the appropriate current intensity (360A). Then, the bulge fracture heights of the samples were recorded for each test. By comparing the bulge fracture height with the state without applying an electric current, the current parameters yielding the maximum bulge fracture height were selected as the appropriate current parameters for the equibiaxial tension stress state. The bulge fracture height with a

current intensity higher and lower than 360A was less than the bulge fracture height of the state without applying an electric current. In our previous study [30], it was observed that by applying electric current with different current parameters, the electroplastic effect had a different effect on formability in uniaxial tension stress state. In addition, in a series of current parameters, applying electric currents reduced formability. In all the hydraulic bulge tests, by applying electric currents, only the intensity of the current was changed as stated. In all the tests, the pulse duration was 20ms and the pulse period was  $120\mu s$ . Each test was conducted twice to ensure the accuracy. The results indicated that the appropriate current parameters in the equibiaxial tension stress state are equal to those of the uniaxial tension stress state. These results are shown in Table 4. The minimal value of standard deviations showed a low measurement error, indicating that the measurement values were close together. Since the appropriate current parameters did not change with the change in the stress state, it can be concluded that the appropriate current parameters do not change with the change of the stress state. This result was also observed in the study conducted by Ghiotti et al. [23]. It should be noted that the same electric current parameters in the uniaxial stress and equibiaxial stress states make a more accurate comparison about the electroplastic effect on the sample formability in these two stress states. As a suggestion for future studies at the end of this article, finding the optimal current parameters through experimental design is recommended.

# 3.2. Experimental Measurement of Fracture Parameters

In our previous study [30], by examining the images of the fracture surface with SEM images, it was concluded that due to the presence of dimples in the fracture surface, for both states of with and without applying an electric current at appropriate current parameters, the type of annealed aluminum 6061 fracture was ductile. In 2008, Bai and Wiersbicki [32] experimentally showed that ductile fracture for aluminum alloys and other metals was related to the third invariant of deviatoric stress which could be expressed by the lode angle.

Table 4
Appropriate current parameters of the hydraulic bulge test for the equibiaxial tension stress state.

Test	Current		Bulge height (mm)						Fracture pressure (bar)					
number	intensity	Iteration	Iteration 1 2 Average Standard		Iteration	1	2	A	Standard					
	(A)	Iteration	1	2	Average	deviation	iteration	1	4	Average	deviation			
1	No current		16.28	16.32	16.3	0.02		75	75	75	0			
2	260		10.35	10.33	10.34	0.01		50	50	50	0			
3	360		17.19	17.21	17.20	0.01		70	70	70	0			
4	460		9.13	9.11	9.12	0.01		75	75	75	0			

According to these cases, the plastic strain at the threshold of fracture could be written as a function of three parameters and in the form of Eq. (1).

$$\bar{\varepsilon}_D^{pl}(\eta, \xi(\theta), \bar{\varepsilon}^{pl})$$
 (1)

where  $\eta$  represents the stress triaxiality,  $\xi(\theta)$  is a function of the lode angle, and  $\bar{\varepsilon}^{pl}$  is the equivalent plastic strain. These fracture parameters are obtained using the following relations [33].

$$\eta = \frac{\beta + 1}{\sqrt{3(\beta^2 + \beta + 1)}} \tag{2}$$

$$\xi(\theta) = \frac{-3\sqrt{3}}{2} \left( \frac{\beta (\beta + 1)}{(\beta^2 + \beta + 1)^{1.5}} \right) \tag{3}$$

$$\bar{\varepsilon}^{pl} = \frac{2\varepsilon_1}{\sqrt{3}} \sqrt{\beta^2 + \beta + 1} \tag{4}$$

where  $\beta$  is calculated from Eq. (5), where  $\varepsilon_1$  and  $\varepsilon_2$ are maximum and minimum plane strains, respectively. These strains were obtained after performing the tests using the method of circular grid analysis on the sample. In this method, as shown in Fig. 6, the circles engraved on the samples in the deformation zone become ellipses, and the maximum and minimum plane strains are calculated using Eqs. (6) and (7).

$$\beta = \frac{\varepsilon_1}{\varepsilon_2}$$
 (5) 
$$\varepsilon_1 = \ln(a/d)$$
 (6)

$$\varepsilon_1 = \ln(a/d)$$
 (6)

$$\varepsilon_2 = \ln(b/d)$$
 (7)

where, as shown in Fig. 6, d is the initial diameter of the circle, and a and b are major and minor diameters of the ellipse, respectively.

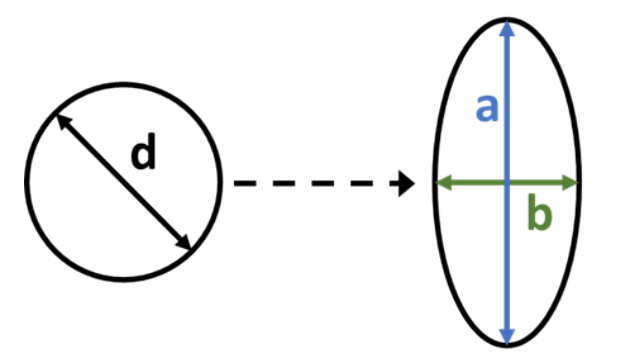


**Fig. 6.** Change of the circle to the ellipse after deformation.

After analyzing the circular patterns, the fracture parameters for the equibiaxial tension stress state for two conditions, without applying an electric current and with applying an electric current at appropriate current parameters, were obtained by Formulas (2) to (7). In order to measure major and minor diameters of the ellipse in this study, Mitutoyo 500-197-20 digital caliper with the accuracy of 0.01mm was used.

# 3.3. Electroplastic Effect on Fracture Parame-

As mentioned in Section 3.1, the hydraulic bulge test was repeated twice for both conditions of with and without applying an electric current at appropriate current parameters. First, in order to calculate fracture parameters, the diameters of a and b (corresponding to Fig. 6) in each sample were measured for the closest circle to the fracture site, which was transformed into an ellipse after deformation. Then, the average of these diameters was calculated. By using Formulas (2) to (7), the fracture parameters for the hydraulic bulge test samples were calculated and the results are shown in Table 5. As can be seen in Table 5, the stress triaxiality and the lode angle remained constant for both conditions of with and without applying a current at appropriate current parameters. Therefore, the electroplastic effect did not affect the state of stress. The fracture equivalent plastic strain as a result of the utilization of electrical pulse was increased by 3.36%, indicating some improvement in formability. In our previous study [30], the electroplastic effect on the formability of AA6061 in the uniaxial tension stress state was investigated in the appropriate current parameters. It was concluded that the fracture strain of the annealed the sample in the uniaxial tension stress state was increased by 23.4%. This shows that in both stress states of equibiaxial and uniaxial tensions, with the utilization of electrical pulses in the same appropriate current parameters, the formability increased. The value of increase in formability in the stress state of uniaxial tension was greater than that of the equibiaxial tension stress state. Considering the fact that the stress triaxiality in the uniaxial tension stress state was less than that of the equibiaxial tension stress state [34], it could be stated that with increasing the stress triaxiality, the amount of electroplastic effect on improving the formability decreased. It should be noted that this result was also observed in the study by Ghiotti, et al. [23].

Table 5 Diameters of a and b (Fig. 6) measured for the closest ellipse to the fracture site and the fracture parameters for the equibiaxial tension stress state correspond to two conditions of with and without applying an electric current at appropriate current parameters.

	Sam	Sample 1		ple 2	Fracture parameters					
	$\overline{a}$	b	$\overline{a}$	b	$a_{\text{average}}$	$b_{\text{average}}$	$\eta$	$\xi(\theta)$	$ar{arepsilon}^{pl}$	
No current	3.63	3.63	3.61	3.61	3.62	3.62	0.67	-1	1.19	
Appropriate current parameters	3.70	3.70	3.69	3.69	3.695	3.695	0.67	-1	1.23	

# 3.4. Electroplastic Effect on Sample Dome Bulge Height

As mentioned in Section 3.1, the hydraulic bulge test was repeated twice for the conditions of with and without applying an electric current at appropriate current parameters. As described in Section 2, the height of the bulge dome was measured for each sample during the test at different pressures by means of a digital caliper. Moreover, the pressure was measured by means of a hand manometer, which was placed before the fluid entered the blank holder. Then, the average height of the bulge dome for each sample was calculated in the two states. These results are shown in Table 6. The minimal value of standard deviations showed a low measurement error, indicating that the measurement values were close together. The diagram depicting changes in the hydraulic bulge pressure in relation to the sample's average bulge dome height is shown in Fig. 7. In the case of without a current, the average bulge dome height at the failure moment was 16.3mm and the failure pressure was 75 bar. Under the condition of utilization of electrical pulses in the appropriate current parameters, the average bulge dome height at the failure moment was 17.2mm and the failure pressure was 70 bar. Therefore, under the electroplastic effect in the appropriate current parameters, the average height of the dome was increased by 5.52%, and the fracture pressure was decreased by 6.67%. According to Fig. 7, by applying an electric current at appropriate current parameters, the average bulge dome height of the sample at the same pressure was higher than that in the case where no pulse current was applied. Fig. 8 shows the hydraulic bulge test samples. Fig. 8a and 8c display the hydraulic bulge test samples in the state of without the utilization of electric pulses, and Fig. 8b and 8d demonstrate the hydraulic bulge test samples in the state of the utilization of electric pulses with appropriate current parameters.

### 3.5. Electroplastic effect on thickness distribution

As mentioned in Section 3.1, the hydraulic bulge test was repeated twice for the conditions of with and without applying an electric current at appropriate current parameters. Fig. 9 indicates the average thickness distribution curve of the two samples in the hydraulic bulge test. The average thickness of the bulge dome was 0.58mm in the state of without applying an electric current and 0.54mm for the state of applying electrical pulses with appropriate current parameters. This means that the average thickness of the sample in the dome of the hydraulic bulge test sample was decreased by 6.9% under the electroplastic effect. Fig. 10 shows the cut picture of the hydraulic bulge test samples. Fig. 10a and 10c exhibit the hydraulic bulge test sample cut image in the state of without the utilization of electric pulses, and Figs. 10b and 10d show the hydraulic bulge test sample cut image for the state of utilization of electric pulses in the appropriate current parameters. By comparing Figs. 10c and 10d qualitatively, in the state of utilizing electric pulses in the appropriate current parameters (Fig. 10d), the thinning of the sheet thickness was greater, especially at the dome bulge sample. Moreover, the sample was stretched more at fracture moment than in the case of without utilization of electric pulses (Fig. 10c).

Table 6

The height of the bulge dome at different pressures for each sample for the states of with and without a current at appropriate current parameters.

		Pressure (bar)							
		12.5	25	40	50	60	70	75	
	Sample 1, bulge dome height (mm)	4.90	6.19	7.05	8.1	9.78	12.61	16.28	
No current	Sample 2 bulge dome height (mm)	4.86	6.23	7.07	8.08	9.76	12.57	16.32	
	Average	4.88	6.21	7.06	8.09	9.77	12.59	16.3	
	Standard deviation	0.02	0.02	0.01	0.01	0.01	0.02	0.02	
Appropriate	Sample 1, bulge dome height (mm)	4.88	6.51	7.50	9.99	13.25	17.19		
current parameters	Sample 2, bulge dome height (mm)	4.92	6.55	7.48	9.95	13.27	17.21		
	Average	4.9	6.53	7.49	9.97	13.26	17.2		
	Standard deviation	0.02	0.02	0.01	0.02	0.01	0.01		

### 3.6. Experimental Stress Strain Curve

The stress strain curve, using the hydraulic bulge test parameters stated in Section 2 and the formulas provided by Hill [35], was achieved as follows. In all the equations, the average bulge dome height was used for  $h_b$ . Eq. (8) shows the relation for bulge radius, proposed by Hill [35].

$$R_b = \frac{d^2_d + 4h^2_b}{8h_b} \tag{8}$$

Eq. (9) represents the relation for computing the instantaneous dome apex sheet thickness proposed by Hill [35].

$$t = t_0 \left( \frac{1}{1 + \left(\frac{h_b}{R_d}\right)^2} \right)^2 \tag{9}$$

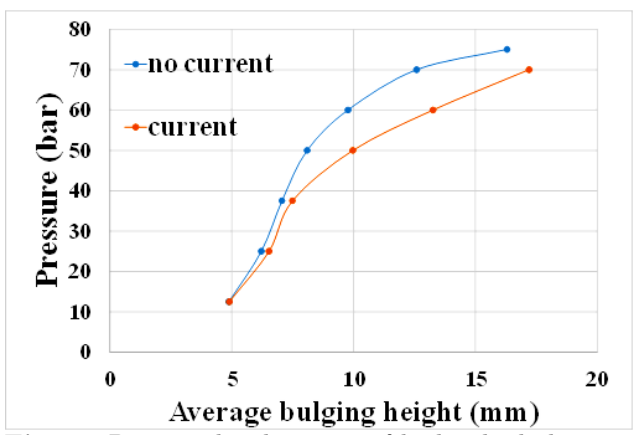


**Fig. 7.** Pressure-height curve of hydraulic bulge test samples.

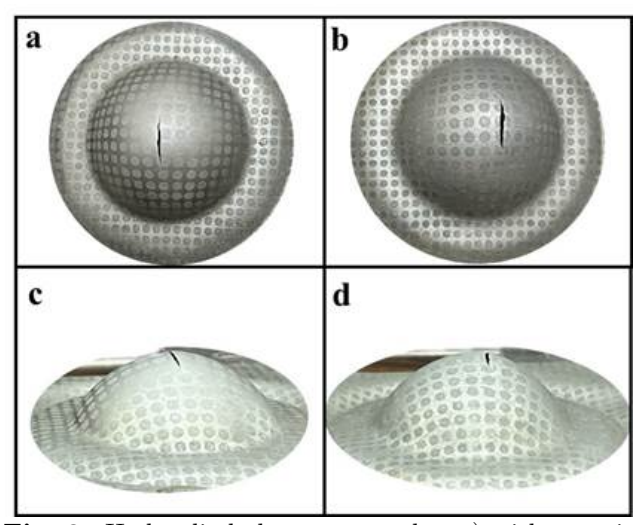


Fig. 8. Hydraulic bulge test samples, a) without utilization of electric pulse from the top view, b) with utilization of electric pulse at appropriate current parameters from the top view, c) without utilization of electric pulses from the front view, d) with utilization of electric pulses at appropriate current parameters from the front view.

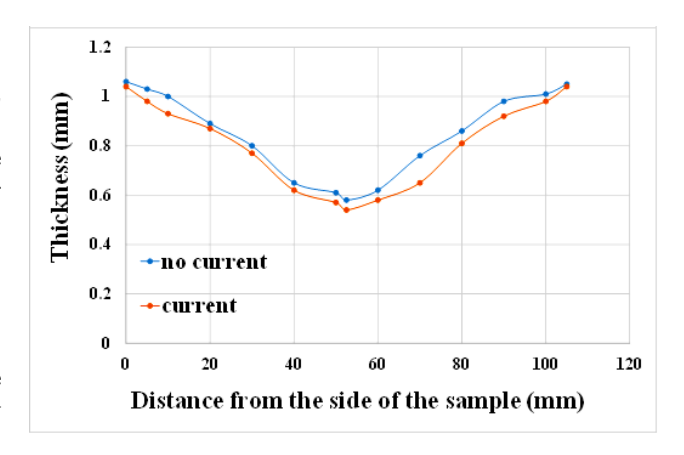


Fig. 9. Average thickness dispensation diagram of hydraulic bulge test samples.

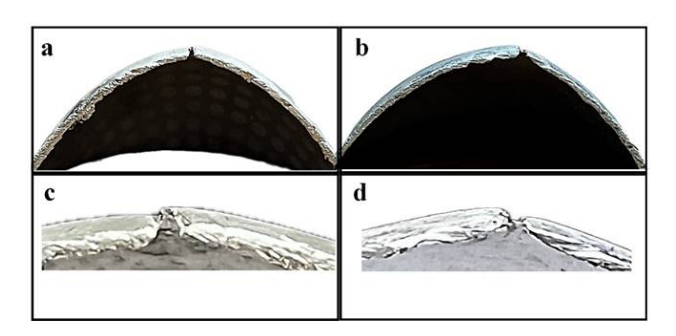


Fig. 10. Cut picture of hydraulic bulge test samples a) without utilization of electric pulse from the front view, b) with utilization of electric pulse at appropriate current parameters from the front view, c) without utilization of electric pulse from the front view with 5x zoom, d) with utilization of electric pulse at appropriate current parameters from the front view with 5x zoom.

To compute the stress-strain curve for the AA6061 sheet in the equibiaxial tension stress state, the classical membrane theory was applied. The stress component in the vertical direction to the sheet surface was not discussed ( $\sigma_z = 0$ ) because the proportion of sheet thickness to its radius was extremely low (t/Rd << 0.1). Taking into account Tresca's yield criterion, Gutscher et al. [36] presented a formula to compute the effective biaxial stress emerged from the hydraulic bulge test. This formula is shown in Eq. (10).

$$\bar{\sigma}_b = \frac{p}{2} \left( \frac{R_b}{t} + 1 \right) \tag{10}$$

Dome Principal strains are:  $\varepsilon_{\Theta}$ ,  $\varepsilon_{\phi}$ , and  $\varepsilon_{t}$ . By supposing the von Mises yield criterion and letting  $\varepsilon_{\Theta} = \varepsilon_{\phi}$ , the effective biaxial strain can be computed as follows:

$$\bar{\varepsilon}_b = \sqrt{\frac{2}{9} \left[ \left( \varepsilon_{\Theta} - \varepsilon_{\phi} \right)^2 + \left( \varepsilon_{\Theta} - \varepsilon_t \right)^2 + \left( \varepsilon_{\phi} - \varepsilon_t \right)^2 \right]}$$
 (11)

Owing to the principle of volume constancy, it is known that there is no volume change as a result of plastic deformation ( $\varepsilon_{\Theta} + \varepsilon_{\phi} + \varepsilon_{t} = 0$ ). Hence, the effective strain can be obtained from Eq. (12).

$$\bar{\varepsilon}_b = \varepsilon_{\Theta} + \varepsilon_{\phi} = -\varepsilon_t = \ln \frac{t_0}{t}$$
 (12)

By placing the data obtained from hydraulic bulge test in the state of equibiaxial tension and using Eqs. (8) and (9), the dome apex bulge radius and the dome apex bulge thickness were obtained. Using Eqs. (10) and (12), the true stress strain curve in the equibiaxial tension stress state was obtained for the two cases of with and without applying an electric current at appropriate current parameters, which is shown in Fig. 11. In this curve, the vertical axis of the biaxial stress and the horizontal axis of the strain are along the thickness of the sample. According to the diagram, by applying the electric current at appropriate current parameters. higher strains were achieved at lower stresses than in the case of without applying an electric current. This shows that by applying an electric current at appropriate current parameters with a lower force, the sheet became thinner. In simpler terms, the sample exhibited more pronounced bulging.

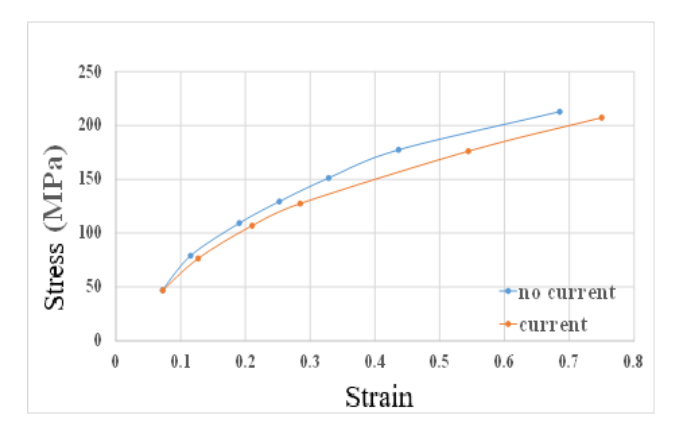


Fig. 11. The true stress strain curve in the equibiaxial tension stress state for the two cases of with and without applying an electric current at appropriate current parameters.

#### 4. Conclusions

In our previous study [30], by studying the electroplastic effect on the formability of AA6061 at appropriate current parameters, it was shown that due to the electroplastic effect, the formability of the annealed sample was increased by 23.4%. In this study, the electroplastic effect in the equibiaxial tension stress state was investigated through the hydraulic bulge test in the annealed heat treatment state. At first, the appropriate current parameters for this stress state were found.

Then, the hydraulic bulge was executed for both without and with the application of a current to the appropriate current parameters. By analyzing the circular patterns created on the samples, the failure parameters were calculated for the stress state of equibiaxial tension. The conclusions of this research are as follows:

- The appropriate current parameters in this stress state are the same as the uniaxial tension state.
- The fracture plastic strain parameter was increased by 3.36%.
- The fracture pressure was decreased by 6.67%.
- The average bulge dome height was increased by 5.52%.
- The average bulge dome thickness was decreased by 6.9%.
- By analyzing the circular patterns created on the samples, the failure parameters were calculated for the stress state of equibiaxial tension. Among the failure parameters, the stress triaxiality and the lode angle were not changed owing to the utilization of electric pulses, and the electroplastic effect had no effect on them.
- Owing to the utilization of electric pulses, it was found that in both stress states of equibiaxial tension and uniaxial tension, the formability was increased and the forming force was decreased with the utilization of electric pulses.
- The amount of increase in formability in the uniaxial tension state was more than that of the equibiaxial tension state.
- Considering that the stress triaxiality in the uniaxial tension state was less than that of the equibiaxial tension state, it can be said that with increasing the stress triaxiality, the amount of electroplastic effect on improved formability decreased.
- Finally, by using the formulas presented in Section ??, the biaxial stress curve is shown in terms of thickness strain. According to this curve, by applying an electric current, the formability of the sample was increased and the forming force was decreased.
- According the results obtained in Section ??, the theoretical results confirmed the experimental results.

As a future work, an experimental design will be carried out in order to investigate the effect of important process parameters on the electroplastic effect on the plastic behavior of annealed aluminum alloy 6061

in more complex stress states. Also, given the fact that the stress states in industrial process are more complex than the uniaxial and equibiaxial tensile stress states, the study of the electroplastic effect on the formability of aluminum alloy 6061 in more stress states could be a basis for the industrialization of forming with the help of electric currents.

### References

- [1] A.E. Tekkaya, N.B. Khalifa, G. Grzancic, R. Hölker, Forming of lightweight metal components: need for new technologies, Procedia Eng., 81 (2014) 28-37.
- [2] M. Elyasi, V. Modanloo, H. Talebi Ghadikolaee, F. Ahmadi Khatir, B. Akhoundi, Investigating the effect of heat treatment in hydraulic rotary draw bending of AA6063 tubes, Modares Mechanical Engineering, 23 (2023) 257-264.
- [3] T. Kuwabara, T. Mori, M. Asano, T. Hakoyama, F. Barlat, Material modeling of 6016-O and 6016-T4 aluminum alloy sheets and application to hole expansion forming simulation, Int. J. Plast., 93 (2017) 164-186.
- [4] K. Mori, P.F. Bariani, B.-A. Behrens, A. Brosius, S. Bruschi, T. Maeno, M. Merkiein, J.J.C.A. Yanagimoto, Hot stamping of ultra-high strength steel parts, CIRP Annals, 66(2) (2017) 755-777.
- [5] M. Elyasi, V. Modanloo, F. AhmadKkhatir, H. Talebi-Ghadikolaee, Experimental investigation of the formability of heat treated AA6063 tubes using hydraulic rotary draw bending process, J. Solid Fluid Mech., 13(4) (2023) 95-106.
- [6] F. Ahmadi khatir, M.H. Sadeghi, P. Fallahi, Journal Of Applied and Computational Sciences in Mechanics 36 (2024) 15-28.
- [7] S. Bruschi, T. Altan, D. Banabic, P.F. Bariani, A. Brosius, J. Cao, A. Ghiotti, M. Khraisheh, M. Merklein, esting and modelling of material behaviour and formability in sheet metal forming, A.E. Tekkaya, CIRP Annals, 63(2) (2014) 727-749.
- [8] S.E. Seyyedi, M. Bakhshi-Jooybari, H. Gorji, M.J. Mirnia, An Experimental and Numerical Investigation of Deformation Mechanics on Hole-Flanging Process of AA6061-T6 Sheets through Single-Point Incremental Forming, J. Stress Anal., 6(1) (2021) 29-46.
- [9] A.J.S. Egea, H.A.G. Rojas, D.J. Celentano, J.A. Travieso-Rodríguez, J.L. i Fuentes,

- Electroplasticity-assisted bottom bending process, J. Mater. Process. Technol., 214(11) (2014) 2261-2267.
- [10] H.D. Nguyen-Tran, H.S. Oh, S.T. Hong, H.N. Han, J. Cao, S.H. Ahn, D.M. Chun, A review of electrically-assisted manufacturing, International Journal of Precision Engineering and Manufacturing-Green Technology, 2 (2015) 365-376.
- [11] H. Conrad, Electroplasticity in metals and ceramics, Mater. Sci. Eng. A, 287(2) (2000) 276-287.
- [12] J.T. Roth, I. Loker, D. Mauck, M. Warner, S. Golovashchenko, A. Krause, Enhanced formability of 5754 aluminum sheet metal using electric pulsing, Transactions of the North American Manufacturing Research Institution of SME, 36 (2008) 405-412.
- [13] J.C. Heigel, J.S. Andrawes, J.T. Roth, M.E. Hoque, R.M. Ford, the North American Manufacturing Research Institute of SME (2005).
- [14] W.A. Salandro, J.T. Roth, Formation of 5052 aluminum channels using electrically-assisted manufacturing (EAM), In International Manufacturing Science and Engineering Conference, 43628 (2009) 599-608.
- [15] A.D. Pleta, M.C. Krugh, C. Nikhare, J.T. Roth, ASME (2013).
- [16] M.J. Kim, K. Lee, K.H. Oh, I.S. Choi, H.H. Yu, S.T. Hong, H.N. Han, Electric current-induced annealing during uniaxial tension of aluminum alloy, Scr. Mater., 75 (2014) 58-61.
- [17] J.H. Roh, J.J. Seo, S.T. Hong, M.J. Kim, H.N. Han, J.T. Roth, The mechanical behavior of 5052-H32 aluminum alloys under a pulsed electric current, Int. J. Plast., 58 (2014) 84-99.
- [18] S.-T. Hong, Y.-H. Jeong, M.N. Chowdhury, D.-M. Chun, M.-J. Kim, H.N. Han, Feasibility of electrically assisted progressive forging of aluminum 6061-T6 alloy, CIRP Annals, 64 (2015) 277-280.
- [19] Z. Xu, G. Tang, S. Tian, F. Ding, H. Tian, Research of electroplastic rolling of AZ31 Mg alloy strip. Journal of materials processing technology, J. Mater. Process. Technol., 182(1-3) (2007) 128-133.
- [20] G. Tang, J. Zhang, M. Zheng, J. Zhang, W. Fang, Q. Li, Experimental study of electroplastic effect on stainless steel wire 304L, Mater. Sci. Eng. A, 281(1-2) (2000) 263-267.
- [21] K. Zhao, R. Fan, Journal of Engineering Materials and Technology, Transactions of the ASME 138 (2016).

- [22] D. Shaffer, S. Sehman, I. Ragai, J.T. Roth, B. Wang, Effect of Electrical Current on Cold Work in Aluminum 2024, In ASME International Mechanical Engineering Congress and Exposition, American Society of Mechanical Engineers, 58493 (2017).
- [23] A. Ghiotti, S. Bruschi, E. Simonetto, C. Gennari, I. Calliari, P. Bariani, Electroplastic effect on AA1050 aluminium alloy formability, CIRP Annals, 67(1) (2018) 289-292.
- [24] E. Simonetto, S. Bruschi, A. Ghiotti, Electroplastic effect on AA1050 plastic flow behavior in H24 tempered and fully annealed conditions, Procedia Manuf., 34 (2019) 83-89.
- [25] W.A. Salandro, J.J. Jones, T.A. McNeal, J.T. Roth, S.-T. Hong, M.T. Smith, Journal of Manufacturing Science and Engineering 132 (2010).
- [26] M.-J. Kim, M.-G. Lee, K. Hariharan, S.-T. Hong, I.-S. Choi, D. Kim, K.H. Oh, H.N. Han, Electric currentssisted deformation behavior of Al-Mg-Si alloy under uniaxial tension, Int. J. Plast., 94 (2017) 148-170.
- [27] D. Dobras, S. Bruschi, E. Simonetto, M. Rutkowska-gorczyca, A. Ghiotti, Materials 14 (2021) 1-14.
- [28] S. Xu, X. Xiao, H. Zhang, Z. Cui, Electroplastic effects on the mechanical responses and deformation mechanisms of AZ31 Mg foils. Materials, 15(4) (2022) 1339-1339.
- [29] H. Eslami, H. G., B.-J. Mohammad, F. Amirhesam, Iranian Journal of Manufacturing Engineering (2024).

- [30] A. Farkhondeh, M. Bakhshi-Jooybari, h. Gorji, M.J. Mirnia, International Journal of Engineering (2024).
- [31] M. Janbakhsh, F. Djavanroodi, M. Riahi, Utilization of bulge and uniaxial tensile tests for determination of flow stress curves of selected anisotropic alloys. Proceedings of the Institution of Mechanical Engineers, Proc. Inst. Mech. Eng., Part L., 227(1) (2013) 38-51.
- [32] Y. Bai, T. Wierzbicki, A new model of metal plasticity and fracture with pressure and Lode dependence, Int. J. Plast., 24(6) (2008) 1071-1096.
- [33] A. Zahedi, B. Mollaei-Dariani, M.J. Mirnia, Experimental Determination and Numerical Prediction of Necking and Fracture Forming Limit Curves of 2024 Aluminum Alloy Sheet Using Damage Criterion, Modares Mechanical Engineering, 17(9) (2017) 361-371.
- [34] M.J. Mirnia, M. Vahdani, Calibration of ductile fracture criterion from shear to equibiaxial tension using hydraulic bulge test, J. Mater. Process. Technol., 280 (2020) 116589-116589.
- [35] R. Hill, C. A theory of the plastic bulging of a metal diaphragm by lateral pressure, The London, Edinburgh, and Dublin Philosophical Magazine and Journal of Science, The London, Edinburgh, and Dublin Philosophical Magazine and Journal of Science, 41(322) (1950) 1133-1142.
- [36] G. Gutscher, H.-C. Wu, G. Ngaile, T. Altan, Determination of flow stress for sheet metal forming using the viscous pressure bulge (VPB) test, J. Mater. Process. Technol., 146(1) (2004) 1-7.